

# Highly Selective Colorimetric/Fluorometric Dual-Channel Fluoride Ion Probe, and Its Capability of Differentiating Cancer Cells

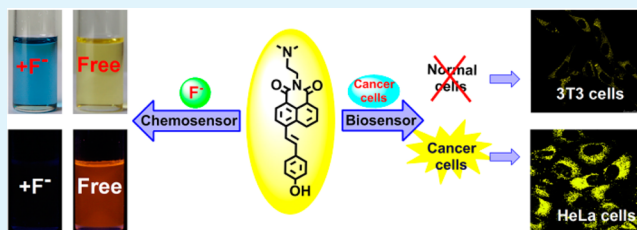
Xujun Zheng,<sup>†,‡</sup> Wencheng Zhu,<sup>†,§</sup> Dong Liu,<sup>#</sup> Hua Ai,<sup>\*,§</sup> Yan Huang,<sup>\*,‡</sup> and Zhiyun Lu<sup>\*,‡</sup>

<sup>‡</sup>Key Laboratory of Green Chemistry and Technology (Ministry of Education), College of Chemistry, <sup>§</sup>National Engineering Research Center for Biomaterials, and <sup>#</sup>College of Materials Science and Engineering, Sichuan University, Chengdu 610064, P. R. China

## Supporting Information

**ABSTRACT:** A dual-channel naphthalimide-based chemosensor for rapid and sensitive detection of fluoride ion has been developed. Upon addition of  $F^-$ , it undergoes deprotonation reaction through H-bonding interactions, and its maximum absorption wavelength is red-shifted for 214 nm to the far-red region, together with drastically quenched fluorescence. In addition, it shows high selectivity toward  $F^-$  anion, thus could be used for practical applications to detecting  $F^-$  in both solution and solid state. Furthermore, the fluorescence of NIM could be enhanced in protein-containing acidic environments, hence NIM could act as lysosome marker to differentiate cancer cells from normal ones in cell imaging.

**KEYWORDS:** fluoride ions, chemosensor, dual-channel, selectivity, cell imaging



acidic environments, hence NIM could act as lysosome marker

Although fluoride ion ( $F^-$ ) is beneficial to dental health and treatment of osteoporosis,<sup>1,2</sup> excessive ingestion of it may result in fluorosis, urolithiasis, and even cancer.<sup>3,4</sup> Therefore, it is important to develop optical probes showing high selectivity,<sup>5–7</sup> good sensitivity,<sup>5,8</sup> and rapid response<sup>5,7,9</sup> toward  $F^-$  ion. Moreover, to act as an ideal  $F^-$  probe, the following features should also be considered: (1) presenting apparent optical signal changes to realize naked-eye detection;<sup>5,10</sup> (2) showing optical response with a huge ratiometric value ( $>200$  nm) to provide more precise built-in correction with minimized environmental effects;<sup>8,11,12</sup> (3) possessing optical signals in far-red to near-infrared (NIR) region ( $>600$  nm) to avoid interference from endogenous chromophores in biological systems;<sup>13–17</sup> (4) showing practical applications to detecting  $F^-$  in real samples.<sup>18</sup> Currently, the construction strategies for  $F^-$  probes are generally based on three kinds of molecular interactions, i.e.,  $F^-$ -induced deprotonation through H-bonding,<sup>7,8,19–23</sup> B–F complexation,<sup>24–26</sup> and  $F^-$ -mediated desilylation of Si–O/Si–C bonds.<sup>5,9,10,12,27–32</sup> However, chemosensors based on B–F complexation mechanism are often sensitive toward oxygen and moisture, and would involve complicated equilibria due to the formation of various fluoroborate species as well;<sup>26</sup> while for chemodosimeters based on desilylation reaction, much excessive  $F^-$  ion is generally needed to reach the saturation of the signal (in some cases, even 1400 equiv.),<sup>27</sup> and the response time is often unsatisfactory.<sup>28</sup>

Consequently, probes based on H-bonding interactions are more attractive. Nevertheless, despite the enormous research efforts,<sup>7,24</sup> most of the H-bonding-based  $F^-$  chemosensors show relatively poor selectivity since they are susceptible to the

interference from alkaline anions like  $AcO^-$ ,  $H_2PO_4^-$ ,  $CN^-$ , and  $OH^-$ .<sup>7,8,33,34</sup> To the best of our knowledge, there have been only two reported examples fulfilling all the aforementioned criteria,<sup>16,19</sup> yet they both only show absorption response toward  $F^-$  anion. Herein, we developed NIM [(E)-2-(2-(dimethylamino)ethyl)-6-(4-hydroxystyryl)-1H-benzo[de]-isoquinoline-1,3(2H)-dione, structure shown in Scheme 1), a novel colorimetric and fluorometric dual-channel naked-eye  $F^-$  probe bearing naphthalimide fluorophore. Different from the frequently used amide/urea/pyrrole binding sites through  $F^- \cdots H-N$  interactions,<sup>8,16,17,19</sup> in NIM, a phenolic OH group is employed as the color-reporting unit through  $F^- \cdots H-O$  interactions. To minimize the cross affinities from interfering alkaline anions, this electron-donating hydroxy group is manipulated to be less acidic by inserting a styryl  $\pi$ -bridge between the donor and acceptor units of NIM. In addition, the resulting D– $\pi$ –A-structured skeleton endows NIM with intramolecular charge transfer (ICT) feature, hence it could display optical response in far-red region after interacting with fluoride ion ( $\lambda_{max} = 641$  nm) due to the much stronger electron-donating capability of phenolate anion than that of phenolic OH group, and a large ratiometric value of  $>200$  nm could even be achieved. Furthermore, NIM possesses good membrane permeability and could accumulate in lysosomes of cells, and hence could differentiate cancer cells from normal ones when used in cell imaging.

Received: March 14, 2014

Accepted: May 15, 2014

Published: May 15, 2014

Scheme 1. Synthetic Routes to NIM

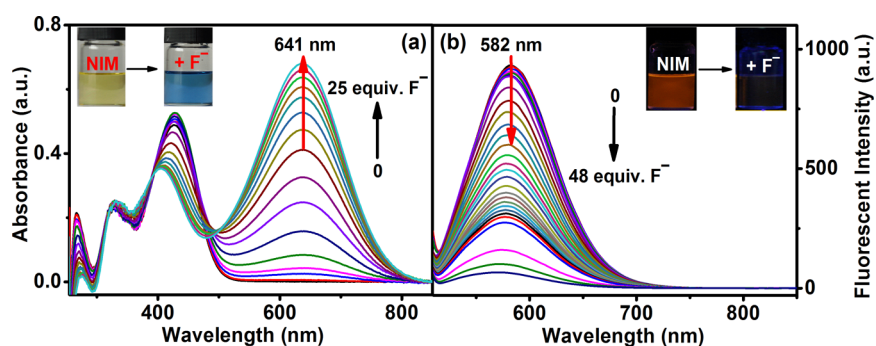
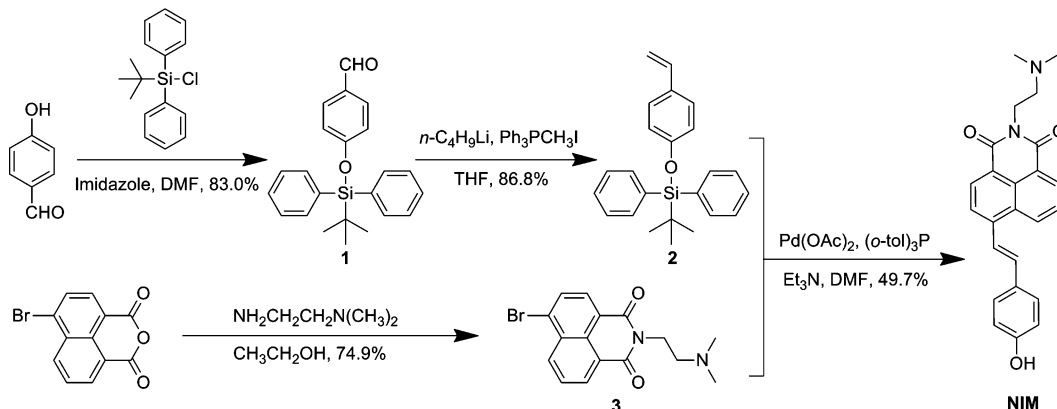


**Figure 1.** (a) UV-vis absorption spectra of NIM ( $20 \mu\text{M}$  in DMSO) upon titration of TBAF (25 equiv.); (b) PL emission spectra of NIM ( $20 \mu\text{M}$  in DMSO) upon titration of TBAF (48 equiv.). Insets: photographs of optical changes upon addition of  $\text{F}^-$ . The excitation wavelength is 490 nm.

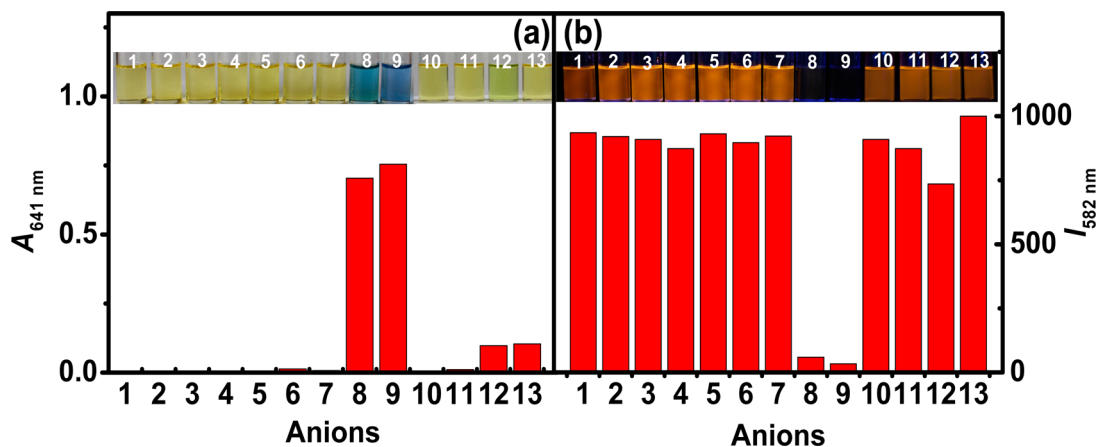


**Figure 2.** (a) Absorption response ( $A_{641 \text{ nm}}$ ) of NIM ( $20 \mu\text{M}$  in DMSO) toward various anions (25 equiv.); (b) Fluorescence response ( $I_{582 \text{ nm}}$ ) of NIM ( $20 \mu\text{M}$  in DMSO) toward various anions (48 equiv.). Insets: photographs of NIM upon addition of various anions. 1, free; 2,  $\text{Cl}^-$ ; 3,  $\text{Br}^-$ ; 4,  $\text{I}^-$ ; 5,  $\text{NO}_3^-$ ; 6,  $\text{H}_2\text{PO}_4^-$ ; 7,  $\text{AcO}^-$ ; 8,  $\text{F}^-$  (TBAF); 9,  $\text{F}^-$  (KF); 10,  $\text{SO}_4^{2-}$ ; 11,  $\text{BF}_4^-$ ; 12,  $\text{CN}^-$ ; 13,  $\text{OH}^-$ .

Spectrometric characterization results indicated that with increasing concentration of tetrabutylammonium fluoride (TBAF), the absorption band of NIM with  $\lambda_{\text{max}} = 427 \text{ nm}$  was weakened gradually, while the newly emerged absorption band with  $\lambda_{\text{max}} = 641 \text{ nm}$  was intensified concurrently, resulting in a huge ratiometric value of 214 nm (Figure 1a). The titration results suggested that the variation of NIM in  $A_{641 \text{ nm}}/A_{427 \text{ nm}}$  correlates almost linearly with the concentrations of the  $\text{F}^-$  ion (see Figure S1a in the Supporting Information). Besides, the addition of  $\text{F}^-$  could also trigger distinct fluorescence quenching of NIM (Figure 1b), and an excellent linearity between fluorescence intensity (at  $\lambda_{\text{em}} = 582 \text{ nm}$ ) and  $\text{F}^-$

concentrations could be observed in the range of 0–48 equiv. ( $960 \mu\text{M}$ ) (see Figure S1b in the Supporting Information). Accordingly, the detection limit was determined to be  $14.2 \mu\text{M}$  (see Figure S2 in the Supporting Information), which was much lower than that of the enforceable drinking water standard for  $\text{F}^-$  ( $210 \mu\text{M}$ ) set by the United States Environmental Protection Agency (EPA). Moreover, the intensity of both absorption ( $\lambda_{\text{max}} = 641 \text{ nm}$ ) and photoluminescence (PL) emission ( $\lambda_{\text{max}} = 582 \text{ nm}$ ) bands could reach their saturation values in 15 s (see Figure S3 in the Supporting Information). Therefore, NIM could act as a dual-channel chemosensor for very rapid detection of  $\text{F}^-$  ion.

As illustrated in Figure 2, only  $F^-$  could trigger distinct optical response of **NIM**, whereas other anions like  $Cl^-$ ,  $Br^-$ ,  $I^-$ ,  $NO_3^-$ ,  $H_2PO_4^-$ ,  $AcO^-$ ,  $SO_4^{2-}$ , and  $BF_4^-$  could cause negligible spectroscopic and visual signal changes (Figure 2 and Figure S4 in the Supporting Information). In fact, the presence of more basic  $CN^-$  ion could only lead to slight optical signal changes of **NIM**. More importantly, upon addition of basic  $OH^-$  anions, although the color of **NIM** solution changed instantly from yellow to blue, it faded back from blue to green to yellow within 10 min. Simultaneously,  $OH^-$  anions could also trigger instant PL quenching of **NIM**, yet the fluorescence could be recovered within 10 min (see Figure S5 in the Supporting Information). Hence after 10 min storage,  $OH^-$  ion just showed slight interfering effect. Therefore, **NIM** was demonstrated to be insensitive to the interference from alkaline anions like  $AcO^-$ ,  $H_2PO_4^-$ ,  $CN^-$ , and  $OH^-$ , hence it displayed high selectivity toward  $F^-$  ion. The reason why  $OH^-$  ion could trigger such dynamic optical signal changes on **NIM** is still unclear, and in-depth investigations on the mechanism behind this behavior is in progress.

Accompanied with spectroscopic alterations, the addition of  $F^-$  into **NIM** could also result in distinct color changes from yellow to deep blue as well as fluorescence quenching, which could be easily distinguished by naked-eye (Figure 1). This is further confirmed by the color gradient experiments with **NIM** ( $40 \mu M$ ) in the presence of various  $F^-$  concentrations. As shown in Figure S8a, in the presence of 8 equiv. of  $F^-$  ( $320 \mu M$ ), obvious color changes of **NIM** solution could be discerned, indicating **NIM** could be used for practical estimation of  $F^-$  concentrations conveniently. In addition, by doping **NIM** (0.2 wt %) into poly(methyl methacrylate) (PMMA) matrix, the detection of  $F^-$  could be realized even in solid-state, confirming the practical potential of **NIM** for qualitative detection of  $F^-$  in environmental samples (see Figure S8b in the Supporting Information). Moreover, **NIM** was also demonstrated to be applicable to the detection of  $F^-$  in real samples like toothpastes (see Figure S9 in the Supporting Information), confirming that **NIM** is a promising fluoride ion probe for practical applications.

For the phenolic proton of **NIM**, its NMR signal was found to be located at 9.84 ppm, whereas that of the phenolic proton of 2-ethyl-6-hydroxy-1*H*-benzo[*de*]isoquinoline-1,3(2*H*)-dione, the analogous compound of **NIM** lacking styryl  $\pi$ -bridge was reported to be 11.88 ppm,<sup>35</sup> therefore, **NIM** bearing an extra  $\pi$ -bridge should show weakened acidity. Upon addition of 0.3 equiv. of  $F^-$ , the  $^1H$  NMR signal of the phenolic proton of **NIM** (9.84 ppm) disappeared, but the signals of other aromatic protons remained to be unaltered (see Figure S10 and Figure S11 in the Supporting Information), whereas further addition of  $F^-$  would induce distinct upfield-shifted proton signals of both the phenyl and ethene-1,2-diyl segments (Figure 3), and a new proton signal at 16.44 ppm corresponding to  $[HF_2]^-$  species<sup>19</sup> could be observed in the presence of 2 equiv. of  $F^-$  (see Figure S10 in the Supporting Information). Therefore, **NIM** should first interact with  $F^-$  ion at the phenolic site through H-bonding,<sup>17</sup> followed by  $F^-$ -induced deprotonation into its phenolate anion.

To evaluate the potential bioapplications of **NIM**, we conducted fluorescence microscopy imaging experiments on **NIM**-incubated RAW 264.7 (mouse monocyte macrophage cell line), 4T1 (mouse breast cancer cell line) and HeLa (human cervical cancer cell line) cells in the absence or presence of  $F^-$ . Nevertheless, although **NIM** could stain all the three kinds of

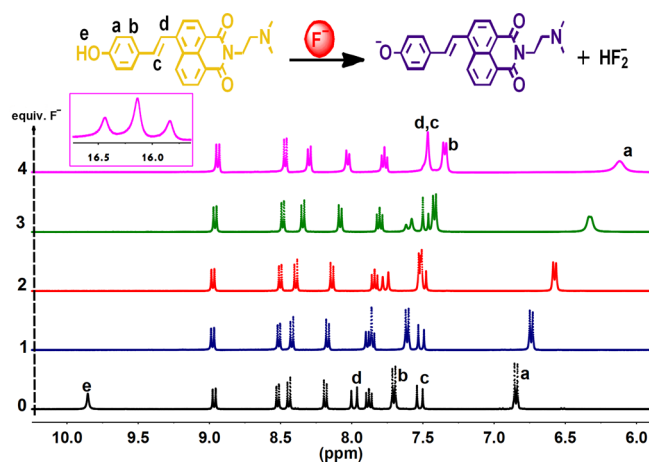


**Figure 3.** Partial  $^1H$  NMR spectral (10.2–5.9 ppm region) changes of **NIM** in  $DMSO-d_6$  in the presence of TBAF (0–4.0 equiv.).

cells, in all the cases, the presence of  $F^-$  ion could not trigger obvious fluorescence quenching in these cells, as shown in Figure S12 in the Supporting Information. More surprisingly, compared to the normal RAW 264.7 cells, the **NIM**-incubated cancerous HeLa and 4T1 cells were found to show much stronger fluorescence (see Figure S12 in the Supporting Information), implying that it might be used to differentiate cancer cells from normal ones in cell imaging applications. This hypothesis was further confirmed by similar experiments on other normal cells like HUVEC (human umbilical vein endothelial cell line), 3T3 (mouse fibroblast cell line) and HEK 293 (human embryonic kidney cell line) and cancer cells like MCF-7 (human breast cancer cell line) (Figure 4 and Figure S13 in the Supporting Information). In depth investigation on intracellular localization of **NIM** revealed that **NIM** could spread in cytoplasm but accumulate in lysosomes of both normal and cancerous cells, since the corresponding fluorescent spots were found to be colocalized with the lysosome markers (LysoTracker, Life Technologies) (see Figure S14 in the Supporting Information). Therefore, as **NIM** could act as lysosome marker, while there exist more numerous, larger lysosomes in cancer cells than normal ones,<sup>36</sup> **NIM**-stained cancer cells could exhibit more intense fluorescence than normal cells, and hence **NIM** could be used to differentiate cancer cells from normal ones in cell imaging applications.

To unveil why **NIM** could act as lysosome marker, we first investigated the fluorescence behaviors of **NIM** in both  $DMSO/H_2O$  (v/v, 75/25) and PBS in neutral and acidic pH environments, since the microenvironments of lysosomes (pH  $\sim$  5) are more acidic than other organelles and cytoplasm.<sup>37</sup> As shown in Figure S15 in the Supporting Information and Figure 5a, **NIM** could emit orange fluorescence in  $DMSO/H_2O$  mixture, but is nearly nonemissive in PBS, but in each case, the fluorescence of **NIM** is insensitive to pH environment variations within pH range of 4.5–7.4. In addition, although when **NIM** was mixed with blank RPMI-1640 medium (pH 7.4), no fluorescence was discernible in this mixture, the addition of fetal bovine serum (FBS) into the medium would result in obvious orange fluorescence whose intensity is in proportion to the concentration of **NIM** (see Figure S16 in the Supporting Information), implying that the fluorescence of **NIM** might be lit up in the presence of protein. To verify this conjecture, we mixed **NIM** with bovine serum albumin (BSA)

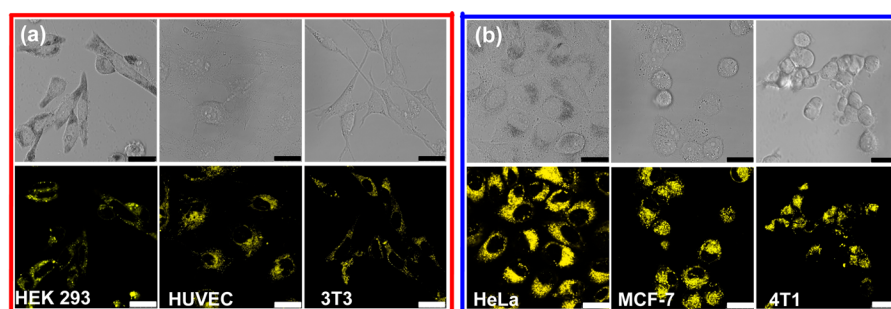


**Figure 4.** Confocal microscopy images of cultured cells incubated with  $7.5 \mu\text{M}$  NIM for 0.5 h. (a) Normal cell examples of HEK 293, HUVEC, and 3T3 cells; (b) Cancer cell examples of HeLa, MCF-7 and 4T1 cells. Scale bar:  $25 \mu\text{m}$ . Top, bright field; bottom, fluorescence.

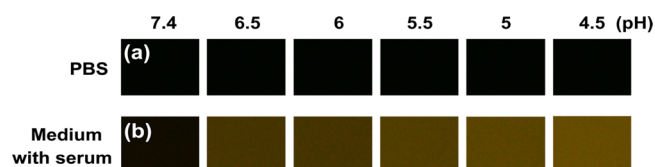


**Figure 5.** (a) Fluorescence of NIM ( $5 \mu\text{M}$ ) in PBS at different pH values.  $100 \mu\text{L}$  NIM-containing PBS was added into a 96-well plate and excited at  $450 \text{ nm}$  under a fluorescence microscope (Leica, Germany); (b) fluorescence of NIM ( $5 \mu\text{M}$ ) in RPMI-1640 with 10% serum at different pH environments. Excited at  $450 \text{ nm}$  under a fluorescence microscope (Leica, Germany).

in PBS (pH 7.4). As shown in Figure S17 in the Supporting Information, the fluorescence intensity of NIM is found to enhance monotonously with increasing BSA concentrations. Therefore, we could draw a conclusion that the presence of protein is related to the enhancement of fluorescence of NIM.

It is noteworthy that the growth medium containing both NIM and serum/BSA is found to display intensified fluorescence upon acidification from pH 7.4 to pH 4.5 (Figure 5b and Figure S18 in the Supporting Information), suggesting that in acidic protein-containing environments, the fluorescence of NIM could be enhanced more effectively. Accordingly, since lysosomes are protein-containing organelles with more acidic microenvironments than those of other organelles and cytoplasm,<sup>37</sup> NIM should show stronger fluorescence in lysosomes comparing to other organelles. To validate this hypothesis, we investigated the fluorescence properties of NIM in both living and dead cells, because lysosomes in living cells display lower pH values than those of dead cells.<sup>37</sup> The results indicated that although NIM could stain both living and dead cells, there exists stronger fluorescence only in the lysosomes of living cells (see Figure S19 in the Supporting Information).

On the basis of all these experimental observations, we tentatively attribute the lysosome-marking capability of NIM to its intensified fluorescence in protein-containing acidic environments. Moreover, as NIM accumulates in lysosomes with acidic microenvironments (pH  $\sim 5$ ), yet in such acidic environments, it should be much difficult for NIM to be deprotonated by  $\text{F}^-$  ion, consequently, NIM displays negligible optical response toward  $\text{F}^-$  ions.

In summary, NIM has been demonstrated to be a high-performance ratiometric colorimetric and “on–off” fluorometric naked-eye  $\text{F}^-$  probe. It shows high selectivity, good sensitivity, and fast response toward  $\text{F}^-$ , and presents absorption signal in far-red region, together with a huge ratiometric value of 214 nm after addition of  $\text{F}^-$  ion. In addition, it could be used for practical applications to detecting

$\text{F}^-$  in both solution and solid state. Furthermore, as the fluorescence intensity of NIM could be enhanced in protein-containing acidic environments, it is a promising lysosome marking reagent, and could be used to differentiate cancer cells from normal ones in cell imaging applications because of the presence of more numerous, larger lysosomes in cancer cells than normal ones.

## ■ ASSOCIATED CONTENT

### Supporting Information

Experimental details, spectroscopic, and cell imaging data, and  $^1\text{H}$  NMR,  $^{13}\text{C}$  NMR, FT-IR, and HRMS spectra. This material is available free of charge via the Internet at <http://pubs.acs.org>.

## ■ AUTHOR INFORMATION

### Corresponding Authors

\*E-mail: huaai@scu.edu.cn.

\*E-mail: huangyan@scu.edu.cn.

\*E-mail: luzhiyun@scu.edu.cn.

### Author Contributions

<sup>†</sup>These authors contributed equally to this work.

### Notes

The authors declare no competing financial interest.

## ■ ACKNOWLEDGMENTS

We acknowledge the financial support for this work by National Key Basic Research Program of China (2013CB933903) and the National Natural Science Foundation of China (Projects 21190031, 21372168, and 51173117). We are grateful to the Analytical & Testing Center of Sichuan University for providing NMR data for the intermediates and objective molecules.

## ■ REFERENCES

- (1) Rakita, P. E. Dentifrice Fluoride. *J. Chem. Educ.* **2004**, *81*, 677–680.
- (2) Kleerekoper, M. The Role of Fluoride in the Prevention of Osteoporosis. *Endocrinol. Metab. Clin. North Am.* **1998**, *27*, 441–452.
- (3) Ayoub, S.; Gupta, A. K. Fluoride in Drinking Water: A Review on the Status and Stress Effects. *Crit. Rev. Environ. Sci. Technol.* **2006**, *36*, 433–487.
- (4) Singh, P. P.; Barjatiya, M. K.; Dhing, S.; Bhatnagar, R.; Kothari, S.; Dhar, V. Evidence Suggesting that High Intake of Fluoride Provokes Nephrolithiasis in Tribal Populations. *Urol. Res.* **2001**, *29*, 238–244.
- (5) Hu, R.; Feng, J.; Hu, D.; Wang, S.; Li, S.; Li, Y.; Yang, G. A Rapid Aqueous Fluoride Ion Sensor with Dual Output Modes. *Angew. Chem., Int. Ed.* **2010**, *49*, 4915–4918.

- (6) Saikia, G.; Dwivedi, A. K.; Iyer, P. K. Development of Solution, Film and Membrane Based Fluorescent Sensor for the Detection of Fluoride Anions from Water. *Anal. Methods* **2012**, *4*, 3180–3186.
- (7) Cametti, M.; Rissanen, K. Recognition and Sensing of Fluoride Anion. *Chem. Commun.* **2009**, *20*, 2809–2829.
- (8) Han, F.; Bao, Y.; Yang, Z.; Fyles, T. M.; Zhao, J.; Peng, X.; Fan, J.; Wu, Y.; Sun, S. Simple Bisthiocarbonohydrazones as Sensitive, Selective, Colorimetric, and Switch-On Fluorescent Chemosensors for Fluoride Anions. *Chem.–Eur. J.* **2007**, *13*, 2880–2892.
- (9) Ke, B.; Chen, W.; Ni, N.; Cheng, Y.; Dai, C.; Dinh, H.; Wang, B. A Fluorescent Probe for Rapid Aqueous Fluoride Detection and Cell Imaging. *Chem. Commun.* **2013**, *49*, 2494–2496.
- (10) Cheng, X.; Li, S.; Xu, G.; Li, C.; Qin, J.; Li, Z. A Reaction-Based Colorimetric Fluoride Probe: Rapid “Naked-Eye” Detection and Large Absorption Shift. *ChemPlusChem*. **2012**, *77*, 908–913.
- (11) Lin, W.; Long, L.; Yuan, L.; Cao, Z.; Chen, B.; Tan, W. A Ratiometric Fluorescent Probe for Cysteine and Homocysteine Displaying a Large Emission Shift. *Org. Lett.* **2008**, *10*, 5577–5580.
- (12) Gai, L.; Chen, H.; Zou, B.; Lu, H.; Lai, G.; Li, Z.; Shen, Z. Ratiometric Fluorescence Chemodosimeters for Fluoride Anion Based on Pyrene Excimer/Monomer Transformation. *Chem. Commun.* **2012**, *48*, 10721–10723.
- (13) Patonay, G.; Antoine, M. D. Near-Infrared Fluorogenic Labels: New Approach to an Old Problem. *Anal. Chem.* **1991**, *63*, 321A–327A.
- (14) Cao, J.; Zhao, C.; Feng, P.; Zhang, Y.; Zhu, W. A Colorimetric and Ratiometric NIR Fluorescent Turn-On Fluoride Chemodosimeter Based on BODIPY Derivatives: High Selectivity via Specific Si–O Cleavage. *RSC Adv.* **2012**, *2*, 418–420.
- (15) Cao, J.; Zhao, C.; Zhu, W. A Near-Infrared Fluorescence Chemodosimeter for Fluoride via Specific Si–O Cleavage. *Tetrahedron Lett.* **2012**, *53*, 2107–2110.
- (16) Bose, P.; Ghosh, P. Visible and Near-Infrared Sensing of Fluoride by Indole Conjugated Urea/Thiourea Ligands. *Chem. Commun.* **2010**, *46*, 2962–2964.
- (17) Saravanan, C.; Easwaramoorthi, S.; Hsiow, C.-Y.; Wang, K.; Hayashi, M.; Wang, L. Benzosenadiazole Fluorescent Probes-Near-IR Optical and Ratiometric Fluorescence Sensor for Fluoride Ion. *Org. Lett.* **2014**, *16*, 354–357.
- (18) Jiang, Y.; Hu, X.; Hu, J.; Liu, H.; Zhong, H.; Liu, S. Reactive Fluorescence Turn-On Probes for Fluoride Ions in Purely Aqueous Media Fabricated from Functionalized Responsive Block Copolymers. *Macromolecules* **2011**, *44*, 8780–8790.
- (19) Xie, Y.; Wang, Q.; Ding, Y.; Li, X.; Zhu, W. Colorimetric Fluoride Sensors Based on Deprotonation of Pyrrole–Hemiquinone Compounds. *Chem. Commun.* **2010**, *46*, 3669–3671.
- (20) Bose, P.; Ahamed, B. N.; Ghosh, P. Functionalized Guanidinium Chloride Based Colourimetric Sensors for Fluoride Andacetate: Single Crystal X-ray Structural Evidence of -NH Deprotonation and Complexation. *Org. Biomol. Chem.* **2011**, *9*, 1972–1979.
- (21) Wang, J.; Hou, Y.; Li, C.; Zhang, B.; Wang, X. Selectivity Tune of Fluoride Ion Sensing for Phenolic OH-Containing BODIPY Dyes. *Sens. Actuators, B* **2011**, *157*, 586–593.
- (22) Sui, B.; Kim, B.; Zhang, Y.; Frazer, A.; Belfield, K. D. Highly Selective Fluorescence Turn-On Sensor for Fluoride Detection. *ACS Appl. Mater. Interfaces* **2013**, *5*, 2920–2923.
- (23) Chetia, B.; Iyer, P. K. 2,6-Bis(2-benzimidazolyl)pyridine as a Chemosensor for Fluoride Ions. *Tetrahedron Lett.* **2008**, *49*, 94–97.
- (24) Zhou, Y.; Zhang, J.; Yoon, J. Fluorescence and Colorimetric Chemosensors for Fluoride-Ion Detection. *Chem. Rev.* **2014**, DOI: 10.1021/cr400352m.
- (25) Liu, Z.; Shi, M.; Li, F.; Fang, Q.; Chen, Z.; Yi, T.; Huang, C. Highly Selective Two-Photon Chemosensors for Fluoride Derived from Organic Boranes. *Org. Lett.* **2005**, *7*, 5481–5484.
- (26) Neumann, T.; Dienes, Y.; Baumgartner, T. Highly Sensitive Sensory Materials for Fluoride Ions Based on the Dithieno[3, 2-b:2',3'-d]phosphole System. *Org. Lett.* **2006**, *8*, 495–497.
- (27) Kim, S. Y.; Hong, J.-I. Chromogenic and Fluorescent Chemodosimeter for Detection of Fluoride in Aqueous Solution. *Org. Lett.* **2007**, *9*, 3109–3112.
- (28) Yang, X.-F.; Qi, H.; Wang, L.; Su, Z.; Wang, G. A Ratiometric Fluorescent Probe for Fluoride Ion Employing the Excited-State Intramolecular Proton Transfer. *Talanta* **2009**, *80*, 92–97.
- (29) Fu, L.; Jiang, F.-L.; Fortin, D. P.; Harvey, D.; Liu, Y. A Reaction-Based Chromogenic and Fluorescent Chemodosimeter for Fluoride Anions. *Chem. Commun.* **2011**, *47*, 5503–5505.
- (30) Kai, Y.; Hu, Y.; Wang, K.; Zhi, W.; Liang, M.; Yang, W. A Highly Selective Colorimetric and Ratiometric Fluorescent Chemodosimeter for Detection of Fluoride Ions Based on 1,8-Naphthalimide Derivatives. *Spectrochim. Acta, Part A* **2014**, *118*, 239–243.
- (31) Sokkalingam, P.; Lee, C.-H. Highly Sensitive Fluorescence “Turn-On” Indicator for Fluoride Anion with Remarkable Selectivity in Organic and Aqueous Media. *J. Org. Chem.* **2011**, *76*, 3820–3828.
- (32) Bao, Y. Y.; Liu, B.; Wang, H.; Tian, J.; Bai, R. A “Naked Eye” and Ratiometric Fluorescent Chemosensor for Rapid Detection of F<sup>-</sup> Based on Combination of Desilylation Reaction and Excited-State Proton Transfer. *Chem. Commun.* **2011**, *47*, 3957–3959.
- (33) Gomez, D. E.; Fabbri, L.; Licchelli, M. Why, on Interaction of Urea-Based Receptors with Fluoride, Beautiful Colors Develop. *J. Org. Chem.* **2005**, *70*, 5717–5720.
- (34) Bordwell, F. G. Equilibrium Acidities in Dimethyl Sulfoxide Solution. *Acc. Chem. Res.* **1988**, *21*, 456–463.
- (35) Sun, W.; Li, W.; Li, J.; Zhang, J.; Du, L.; Li, M. Naphthalimide-Based Fluorescent Off/On Probes for the Detection of Thiols. *Tetrahedron* **2012**, *68*, 5363–5367.
- (36) Saftig, P.; Sandhoff, K. Killing from the Inside. *Nature* **2013**, *502*, 312–313.
- (37) Luzio, J. P.; Pryor, P. R.; Bright, N. A. Lysosomes: Fusion and Function. *Nat. Rev. Mol. Cell Biol.* **2007**, *8*, 622–632.